

1 **Dual antibiotherapy of tuberculosis mediated by inhalable locust bean gum**
2 **microparticles**

3 Susana Rodrigues^{1,2§}, Ana D Alves^{1§}, Joana S Cavaco¹, Jorge F Pontes^{1,2}, Filipa
4 Guerreiro^{1,2}, Ana M Rosa da Costa³, Francesca Buttini⁴ and Ana Grenha^{1,2*}

5
6 ¹Center for Biomedical Research (CBMR), Faculty of Sciences and Technology,
7 University of Algarve, Faro, Portugal; ²Centre for Marine Sciences (CCMar),
8 Faculty of Sciences and Technology, University of Algarve, Faro, Portugal;
9 ³Algarve Chemistry Research Center (CIQA) and Department of Chemistry and
10 Pharmacy, Faculty of Sciences and Technology, University of Algarve, Faro,
11 Portugal; ⁴Department of Food and Drug Science, University of Parma, Parma,
12 Italy; §Authors with equal contribution

13
14 *Corresponding author:

15 University of Algarve

16 CBMR and CCMAR, Faculty of Sciences and Technology

17 Campus de Gambelas

18 8005-139 Faro, Portugal

19 Tel.: +351 289800100 – Ext. 7441

20 Fax: +351 289818419

21 E-mail address: amgrenha@ualg.pt

22

23

24 **Abstract**

25 Despite the existence of effective oral therapy, tuberculosis remains a deadly
26 pathology, namely because of bacterial resistance and incompliance with
27 treatments. Establishing alternative therapeutic approaches is urgent and
28 inhalable therapy has a great potential in this regard. As pathogenic bacteria are
29 hosted by alveolar macrophages, the co-localisation of antitubercular drugs and
30 pathogens is thus potentiated by this strategy. This work proposes inhalable
31 therapy of pulmonary tuberculosis mediated by a single locust bean gum (LBG)
32 formulation of microparticles associating both isoniazid and rifabutin,
33 complying with requisites of the World Health Organisation of combined
34 therapy. Microparticles were produced by spray-drying, at LBG/INH/RFB mass
35 ratio of 10/1/0.5. The aerodynamic characterisation of microparticles revealed
36 emitted doses of more than 90% and fine particle fraction of 38%, thus
37 indicating the adequacy of the system to reach the respiratory lung area, thus
38 partially the alveolar region. Cytotoxicity results indicate moderate toxicity (cell
39 viability around 60%), with a concentration-dependent effect. Additionally, rat
40 alveolar macrophages evidenced preferential capture of LBG microparticles,
41 possibly due to chemical composition comprising mannose and galactose units
42 that are specifically recognised by macrophage surface receptors.

43

44 **Keywords:** inhalation, locust bean gum, microparticles, polysaccharides, spray-
45 drying, tuberculosis therapy

46

47 **1. Introduction**

48 Tuberculosis (TB) remains a leading cause of death, with particular incidence
49 and prevalence in developing countries (WHO, 2016). Drug resistance is a
50 major problem, but therapeutic incompliance is also a great limitation (McBryde
51 et al., 2017). Albeit the commercial availability of several effective oral and
52 parenteral drugs and the existence of international treatment guidelines (NICE,
53 2016; Wells et al., 2009), new therapeutic approaches are demanded not only to
54 improve compliance but also to reduce the severe side effects associated with
55 conventional therapy (Kaur et al., 2016; Lee et al., 2015). Inhalable therapy has
56 great potential in this context, enabling the direct administration of drugs to the
57 alveoli, where macrophages hosting pathogenic bacteria are located (Gupta et
58 al., 2016; Parumasivam et al., 2016).

59 In a previous work, we proposed the use of spray-dried microparticles based on
60 locust bean gum (LBG) as inhalable formulation for the treatment of pulmonary
61 tuberculosis. The individual association of first-line antitubercular drugs was
62 effective and a preliminary assay further suggested high affinity of LBG
63 microparticles for macrophages (Alves et al., 2016), which we explained by
64 specific recognition of the mannose and galactose residues of microparticles by
65 macrophage surface receptors (Ahsan et al., 2002). LBG was proposed in that
66 work for the first time for lung delivery applications. It is a galactomannan and
67 its biodegradability has been ascribed to the presence of β -mannosidase in the
68 lung (Alkhayat et al., 1998).

69 This work intends to produce a dry powder that delivers two antitubercular drugs
70 upon inhalation while providing improved internalisation by macrophages,
71 mediated by LBG. Furthermore, the respirability of LBG microparticles was

72 studied in order to determine their inhalability when used as carriers for
73 antitubercular drugs. The microparticle aerosolisation profile was experimentally
74 determined. The uptake by macrophages was assessed and compared with that of
75 microparticles composed by a polymer devoid of specific moieties recognizable
76 by macrophage receptors. Finally, combined therapy is proposed by the
77 association of two first-line antitubercular drugs (isoniazid and rifabutin) in a
78 single microparticle formulation, to meet the World Health Organisation (WHO)
79 requirements of combined tuberculosis therapy (WHO, 2014).

80

81 **2. Materials and Methods**

82 **2.1. Materials**

83 Locust bean gum (LBG, $C_{30}H_{50}O_{26}$, M_w 860 kDa (Pollard et al., 2008)), poly
84 (vinyl alcohol) (PVA, $[-CH_2CHOH-]_n$, M_w 89-98 g/mol), isoniazid (INH,
85 $C_6H_7N_3O$, M_w 137.14 g/mol), Tween 80[®], phosphate buffer saline (PBS) tablets
86 pH 7.4, Dulbecco's modified Eagle's medium (DMEM), L-glutamine solution
87 (200 mM), non-essential amino acids solution and penicillin/streptomycin
88 (10000 units/mL, 10000 g/mL), trypsin-EDTA solution (2.5 g/L trypsin, 0.5 g/L
89 EDTA), trypan blue solution (0.4%), phorbol 12-myristate 13-acetate (PMA,
90 $C_{36}H_{56}O_8$), thiazolyl blue tetrazolium bromide (MTT), *N*-(3-
91 dimethylaminopropyl)-*N'*-ethylcarbodiimide hydrochloride (EDAC), Triton-X
92 100, sodium dodecyl sulfate (SDS), dimethylformamide (DMF), dimethyl
93 sulfoxide (DMSO) and HCl were purchased from Sigma-Aldrich (Germany).
94 Lactate dehydrogenase (LDH) kit was purchased from Takara Bio (Tokyo,
95 Japan). Rifabutin (RFB, $C_{46}H_{62}N_4O_{11}$, M_w 847.00 g/mol) was supplied by
96 Chemos (Germany) and fetal bovine serum (FBS) by Gibco (Life Technologies,

97 USA). RPMI 1640 and Ham's F12 media were obtained from Lonza Group AG
98 (Switzerland). Ultrapure water (MilliQ, Millipore, UK) was used throughout. All
99 other chemicals were reagent grade.

100

101 **2.2. Cell lines**

102 A549 cells (human alveolar epithelium) and NR8383 cells (rat alveolar
103 macrophages) were obtained from the American Type Culture Collection
104 (ATCC, USA) and used in passages 27-37 and 9-18, respectively. THP-1 cells
105 (human monocytes) were obtained from the Leibniz-Institut DSMZ (Germany)
106 and used in passages 10-20. Cell cultures were grown in humidified 5%
107 CO₂/95% atmospheric air incubator at 37 °C (HerAcell 150, Heraeus,
108 Germany). Cell culture medium (CCM) for A549 cells was DMEM
109 supplemented with 10% (v/v) FBS, 1% (v/v) L-glutamine solution, 1% (v/v)
110 non-essential amino acids solution and 1% (v/v) penicillin/streptomycin. For
111 NR8383 cells, CCM consisted of Ham's F12 supplemented with 15% (v/v) FBS,
112 1% (v/v) L-glutamine and 1% (v/v) penicillin/streptomycin, while THP-1 cells
113 were grown in RPMI 1640 medium supplemented with 10% (v/v) FBS, 1% (v/v)
114 L-glutamine and 1% (v/v) penicillin/streptomycin.

115 THP-1 cells were grown in suspension and cell culture was maintained between
116 0.2×10^6 and 0.8×10^6 cells/mL. When reaching this higher concentration, cells
117 were sub cultivated in new passage at the concentration of 0.2×10^6 cells/mL.
118 Differentiation of THP-1 monocytes to provide the macrophage phenotype was
119 performed using PMA (0.2×10^6 cells/mL, 50 nM, 48 hours exposure), after
120 which the medium was replaced by fresh medium without PMA for 24 hours
121 before the experiments. NR8383 cells grow in mixed culture (half population

122 keeps adherent and half suspended). Adherent cells were those used to perform
123 the assays described below and their harvesting was made by scraping.

124

125 **2.3. Preparation of microparticles**

126 LBG microparticles, without drug and containing an association of the
127 antitubercular drugs INH and RFB, were prepared by spray-drying, according to
128 a previously reported protocol (Alves et al., 2016). The preparation of unloaded
129 LBG microparticles involved grinding LBG in a glass mortar for 10 min, after
130 which 5 mL HCl 0.1 M were slowly added and grinding continued until
131 complete mixture of powder and HCl solution was obtained. This was followed
132 by the addition of purified water previously heated to 85 °C, up to a final volume
133 of 50 mL. The concentration of LBG in the final solution was 2% (w/v). The
134 solution was maintained under magnetic stirring for 30 min and subsequently
135 placed on a water bath at 85 °C under slow stirring for additional 30 min. At the
136 end, the solution was kept under stirring at room temperature overnight, until the
137 moment of spray-drying.

138 For the production of drug-loaded microparticles, a solid dispersion of LBG and
139 RFB was first prepared, by trituration in a mortar. After grinding, the same
140 procedure used to prepare the LBG solution described above was applied. In
141 parallel, INH was triturated in a mortar, being then solubilized with purified
142 water under mild stirring for 10 minutes. The resulting solution was slowly
143 added to the previously formed LBG/RFB solution immediately before spray-
144 drying.

145 Microparticles were produced at LBG/INH/RFB mass ratio of 10/1/0.5 (final
146 concentration of solids is 2.3%, w/v) using a laboratory mini spray dryer (Büchi

147 B-290, Büchi Labortechnik AG, Switzerland) operating in open mode and
148 equipped with a high-performance cyclone. Protection from light was ensured
149 for the whole process. The operating parameters were: inlet temperature: 160 ± 2
150 °C; aspirator setting: 85%; feed rate: 0.7 ± 0.1 mL/min; and spray flow rate: 473
151 L/h. These conditions resulted in outlet temperature of 100 ± 2 °C. After spray-
152 drying, microparticles were collected, placed in a dark flask and stored inside a
153 desiccator until further use.

154 The spray-drying yield was calculated by gravimetry, comparing the total
155 amount of solids initially added with the resultant weight of microspheres after
156 spray-drying (Grenha et al., 2005).

157 Fluorescent (unloaded) microparticles of LBG or PVA were also prepared, to be
158 used in the assay of macrophage capture. Covalent binding between fluorescein
159 and the polymeric molecules was performed before microparticle production. To
160 do so, LBG or PVA (1.0 g) were dissolved in HCl solution (10^{-4} M) at a
161 concentration of 1% (w/v). LBG solution was applied the same treatment
162 described above for the preparation of LBG microparticles. PVA solution was
163 maintained at 80 °C under stirring overnight. Fluorescein (43 mg) was dissolved
164 in ethanol 96% (v/v) and added to the previously formed LBG or PVA solutions.
165 EDAC (ca. 33 mg) was dissolved in milli-Q water and added to the solution.
166 This was kept under stirring for 72 h and then dialysed (2000 Da M_w cut off)
167 against water. Light protection was ensured in the whole process. The resulting
168 suspension was frozen and freeze-dried (FreeZone Benchtop Freeze Dry System,
169 Labconco, USA). The fluorescently-labelled polymers were stored in a
170 desiccator until further use, under light protection. Fluorescent microparticles
171 were produced by spray-drying. The used conditions were the same described

172 above for LBG, while the following were used for PVA: inlet temperature: $155 \pm$
173 $2 \text{ }^\circ\text{C}$; aspirator setting: 80%; feed rate: $1.0 \pm 0.1 \text{ mL/min}$; and spray flow rate:
174 473 L/h . These conditions resulted in outlet temperature of $96 \pm 2 \text{ }^\circ\text{C}$.

175

176 **2.4. Characterisation of microparticles**

177 *2.4.1. Morphology*

178 The surface morphology of LBG microparticles was characterised by field
179 emission scanning electron microscopy (FESEM; FESEM Ultra Plus, Zeiss,
180 Germany). Dry powders were placed onto metal plates and 5 nm thick iridium
181 film was sputter-coated (model Q150T S/E/ES, Quorum Technologies, UK) on
182 the samples before viewing.

183

184 *2.4.2. Feret's diameter*

185 Microparticle size was estimated as the Feret's diameter and was directly
186 determined by optical microscopy (Microscope TR 500, VWR international,
187 Belgium) from the manual measurement of 300 microparticles ($n = 3$).

188

189 *2.4.3. Density*

190 Real density (g/cm^3) was determined using a Helium Pycnometer (Micromeritics
191 AccuPyc 1330, Germany) ($n = 3$). Tap density (g/cm^3) was determined using a
192 tap density tester (Densipro 250410, Deyman, Spain), by measuring the volume
193 of a known weight of powder before and after tapping, respectively ($n = 3$). The
194 determination of tap density involved tapping the sample until no further
195 reduction of powder volume was observed (average of 180 taps).

196

197 *2.4.4. Drug association efficiency and loading*

198 The determination of microparticle drug content was performed by UV-Vis
199 spectrophotometry (Pharmaspec UV-1700, Shimadazu, Japan), at 265.5 nm for
200 INH and 500 nm for RFB. A screening of the matrix material (LBG) revealed no
201 interference at the selected wavelengths.

202 In order to determine the drug content, a certain amount of drug-loaded
203 microparticles was incubated with HCl 0.1 M, under magnetic stirring for 60
204 min, which ensures complete dissolution of the carriers. Samples were then
205 centrifuged (8000 rpm, 30 min; 5810 R, Eppendorf, Germany) and filtered (0.45
206 μm) before quantification. Calibration curves were performed at 265.5 nm for
207 INH and at both this wavelength and at 500 nm for RFB, using the medium of
208 dissolution of unloaded microparticles. The latter curve was used to determine
209 the concentration of RFB and the former allowed the determination of the
210 fraction of the absorbance at 265.5 nm that is due to RFB, the remainder being
211 attributable to INH, thus allowing the determination of its concentration through
212 the corresponding calibration curve. Drug association efficiency (AE) and
213 microparticle (MP) loading capacity (LC) were estimated as follows ($n = 3$):

214 $AE (\%) = (\text{Real amount of drug on MP} / \text{Theoretical amount of drug on MP}) \times$
215 100 (Eq. 1)

216 $LC (\%) = (\text{Real amount of drug on MP} / \text{Weight of MP}) \times 100$ (Eq. 2)

217

218 **2.5. Aerodynamic characterisation of microparticles**

219 HPMC size 3 capsules (Quali-V-I, Qualicaps, Spain) were filled with 22.5 mg of
220 LBG/INH/RFB powder. The content of four capsules was discharged in each
221 aerodynamic test using the medium resistance RS01[®] inhaler (Plastiapae Spa,

222 Italy) and experiments were performed in triplicate. The device was connected to
223 the Andersen cascade impactor (ACI, Copley Scientific, UK) operated at
224 60 L/min, ensuring a pressure drop of 4 kPa through the device. This was
225 activated for 4 s in order to let 4 L of air passing through the system, thus
226 complying with the standard procedure described by USP 38 and Ph.Eur.8
227 (Ph.Eur., 2014; USP, 2015).

228 ACI separates particles according to their aerodynamic diameter and it was
229 assembled using the appropriate adaptor kit for the 60 L/min air flow test. Cut-
230 offs of the stages from -1 to 6 are the following: 8.60, 6.50, 4.40, 3.20, 1.90,
231 1.20, 0.55, 0.26 μm . A glass fiber filter (Whatman, Italy) was placed right below
232 stage 6 in order to collect particles with diameter lower than that of stage 6 cut-
233 off.

234 The plates of the impactor were coated with a thin layer of ethanol containing
235 1% (w/v) Tween 20 to prevent particle bounce. The drugs were recovered from
236 the apparatus with water/acetonitrile mixture (50/50, v/v) and quantified by
237 HPLC (Agilent 1200 series, Germany). A LiChrospher[®] 100 RP-18 (5 μm)
238 column of 4 mm i.d.×250 mm length with security guard cartridge was used.

239 The eluent was a mixture of phosphate buffer pH = 7 (A) and acetonitrile (B) at
240 a flow rate of 1 mL/min, starting with A/B = 95:5 and kept for 5 min, followed
241 by a 7 min step gradient, until a 20:80 A/B ratio was reached, which was then
242 kept for 16 min. Detection was performed by a diode array detector at 275 nm.

243 The used chromatographic conditions were: gradient flow (Phosphate buffer pH
244 = 7 (A), acetonitrile (B); A/B from 95:5 in the first 5 min it is changed to 20:80
245 in 7 min and kept in this 20:80 during other 16 min). A linear calibration plot for
246 INH and RFB was obtained over the range 10-400 $\mu\text{g/mL}$ (n= 3). Under these

247 conditions, the retention times of INH and RFB were 4.7 and 17.4 min,
248 respectively.

249 The quantification of drug deposited inside the impactor allows calculating
250 different aerodynamic parameters. The emitted dose (ED) is the amount of drug
251 ex-device, considered the total amount of drug collected in the impactor,
252 quantified by HPLC (induction port, stages -1 to 6 and filter). The mass median
253 aerodynamic diameter (MMAD) was determined by plotting the cumulative
254 percentage of mass less than the stated aerodynamic diameter on probability
255 scale versus aerodynamic diameter on logarithmic scale. The fine particle dose
256 (FPD) corresponds to the mass of drug particles with aerodynamic diameter
257 lower than 5 μm calculated using the particle size distribution equation obtained
258 from the ACI analysis. The fine particle fraction (FPF) is the ratio between the
259 FPDs and the MD.

260 The drug recovery ranged between 77-91% in all the experiments, being thus
261 coincident with the requisites of the pharmacopeia (Buttini et al., 2013).

262

263 **2.6. Determination of drug release profile**

264 The determination of drug release was performed in PBS pH 7.4 added of 1%
265 (v/v) Tween 80[®]. The assay respected sink conditions, as the maximum amount
266 of drug was always below 30% of its maximum solubility (EMA, 2014). INH
267 solubility was considered 274 ± 4.79 mg/mL (Hiremath and Saha, 2008), while
268 that of RFB was determined experimentally to be 0.496 mg/mL (Alves et al.,
269 2016). A determined amount of microparticles (20 mg) was incubated with the
270 medium (10 mL), at 37 °C, under mild shaking (100 rpm, orbital shaker OS 20,
271 Biosan, Latvia). Samples (1 mL) were periodically collected and the amount of

272 each drug quantified as indicated above (n = 3). Direct quantification applied for
273 RFB, while INH required dilution (1:10). A calibration curve was performed
274 using the medium resulting from the incubation of unloaded LBG
275 microparticles, after centrifugation (8000 rpm, 60 min) and filtration (0.45 µm).

276

277 **2.7. *In Vitro* Biocompatibility Study**

278 **2.7.1. Cell viability evaluation by MTT test**

279 The evaluation of cell viability upon exposure to LBG/INH/RFB microparticles
280 was performed by the MTT assay, using two cell lines of high relevance within
281 the scope of tuberculosis infection, A549 and macrophage-differentiated THP-1
282 cells. A549 cells were seeded at a density of 1×10^4 cells/well on 96-well plates
283 (Orange Scientific, Belgium), in 100 µL of complete DMEM. Cells were
284 incubated for 24 h at 37 °C in 5% CO₂ atmosphere before use. THP-1 cells were
285 differentiated with PMA to obtain the macrophage-phenotype before the
286 experiments, according to the procedure described above, with the necessary
287 adaptations. THP-1 cells were seeded on 96-well plates (0.035×10^6 cells/well)
288 in 100 µL of RPMI supplemented with 50 nM of PMA and incubated for 48 h at
289 37 °C in 5% CO₂ atmosphere. After that time, CCM was renewed for other 24 h,
290 before the experiments.

291 Microparticles (unloaded or drug-loaded) were exposed in the form of a
292 suspension prepared in pre-warmed CCM without FBS and evaluated at the
293 concentrations of 0.1 and 0.5 mg/mL (includes polymers and drugs), for 3 and
294 24 h. INH and RFB were also tested as free drugs, at concentrations representing
295 their loading in microparticles (0.01 and 0.05 mg/mL for INH; 0.005 and 0.025
296 mg/mL for RFB).

297 MTT solution (0.5 mg/mL in PBS, pH 7.4) was added after the exposure time (in
298 A549 cells, samples were previously removed; in THP-1 cells no removal was
299 applied) and incubated for 2 h, after which formazan crystals were solubilised
300 with DMSO (A549 cells) or 10% SDS in a 1:1 mixture of DMF:water (THP-1
301 cells) and the absorbance measured by spectrophotometry (Infinite M200,
302 Tecan, Austria). The viability of untreated cells was assumed to correspond to
303 100% of cell viability, and viability of treated cells was compared to this control.
304 The assay was replicated at least three times, each with six replicates.

305

306 **2.7.2. Determination of cell membrane integrity**

307 The integrity of cell membrane after exposure to LBG microparticles was
308 determined by the quantification of LDH released by cells. This was performed
309 in A549 and macrophage-differentiated THP-1 cells upon 24 h exposure to a
310 concentration of 0.5 mg/mL of unloaded or drug-loaded LBG microparticles.
311 The chosen concentration corresponds to the maximum concentration tested in
312 the MTT assay. Free INH and RFB were also tested as controls (0.05 mg/mL for
313 INH; 0.025 mg/mL for RFB).

314 Cells were cultured in 96-well plates in the conditions described before for the
315 MTT assay (the assays were performed simultaneously). Upon exposure, cell
316 culture supernatants were collected, centrifuged (16 000 x g, 5 min, 4 °C) and
317 processed using a commercial kit. Absorbances were measured by
318 spectrophotometry (Infinite M200, Tecan, Austria) at a wavelength of 490 nm
319 (background correction at 690 nm).

320 A negative control of LDH release was performed incubating cells with CCM
321 only and Triton-X 100 (10%) was used as positive control, being assumed as

322 100% LDH release. Released LDH upon incubation with each sample was
323 determined by comparison with the positive control. All measurements were
324 performed in triplicate.

325

326 **2.8. Macrophage capture of LBG microparticles**

327 The determination of macrophage ability to capture microparticles was
328 determined *in vitro* in two cell lines, differentiated THP-1 cells and NR8383
329 cells. The latter were seeded (1.0×10^6 cells per well) in 6-well plates for
330 adhered cells, with 2 mL of Ham's F12 medium. This procedure was performed
331 24 h before the test to ensure the adhesion of 50 to 75% of the original
332 population. THP-1 cells (2.0×10^5 cells/mL) were suspended in RPMI medium
333 supplemented with 50 nM PMA and seeded at 5 mL/well in 6-well plates for
334 cells in suspension.

335 The evaluation of microparticle uptake by macrophages was performed by flow
336 cytometry (FacScalibur cell analyser, BD Biosciences, Belgium) upon exposure
337 to LBG and PVA microparticles ($50 \mu\text{g}/\text{cm}^2$), both fluorescently-labelled. PVA
338 microparticles were used as control. Microparticles were aerosolised onto the
339 macrophage layer using the Dry powder Insufflator™ (Model DP-4, Penn-
340 Century™, USA) and 2 hours incubation at 37 °C was allowed, without CCM
341 (only a residual amount of medium was kept to ensure the hydration of cell
342 surface). The phagocytic process was stopped by the addition of a cold solution
343 of PBS.3% FBS (5 mL, two applications), which also provided washing. Cells
344 were scraped and centrifuged (1500 rpm, 2 min, room temperature, centrifuge
345 MPW – 223e, MedInstruments, Poland) in 2 mL of PBS.3% FBS. The cycle of
346 resuspension in PBS.3% FBS and centrifugation was repeated thrice. At the end,

347 cells were re-suspended in 1 mL of PBS.3% FBS, transferred to cytometry tubes
348 (BD Biosciences, Belgium) and maintained at 4 °C until the analysis.

349 In flow cytometry, FSC-H and SSC-H channels were used, respectively, to
350 measure size and granularity of cells, while side scatter light was used to identify
351 cell viable population. The amount of cells exhibiting a fluorescent signal was
352 considered to have phagocytosed microparticles. The assay for each dose was
353 replicated at least three times.

354

355 **2.9. Statistical analysis**

356 The student t-test and the one-way analysis of variance (ANOVA) with the
357 pairwise multiple comparison procedures (Holm-Sidak method) were performed
358 to compare two or multiple groups. For the analysis of results of in vitro release
359 assay, a two-way ANOVA with Bonferroni's method for multiple comparison
360 test was used. All analysis were run using the GraphPad Prism (version 6.07)
361 and differences were considered to be significant at a level of $p < 0.05$.

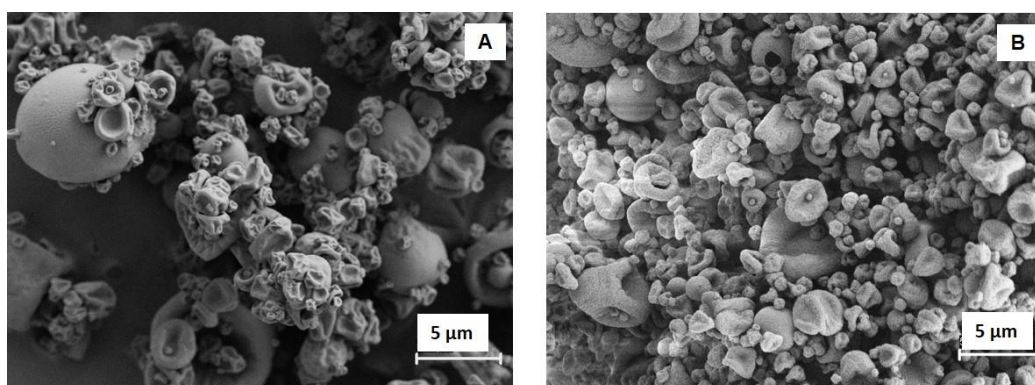
362

363 **3. Results and Discussion**

364 **3.1. Preparation and characterisation of LBG/INH/RFB microparticles**

365 LBG microparticles loaded with a combination of the first-line antitubercular
366 drugs INH and RFB were successfully obtained by spray-drying, with yields of
367 60-70%. The used concentration of LBG (2%, w/v) was chosen from previous
368 experiments (unpublished data) in order to provide suitable microparticle size
369 for the purpose of lung delivery, along with acceptable spray-drying yield.
370 Theoretical drug loadings of 8.70% (INH) and 4.35% (RFB) were selected
371 because they provide microparticles without the formation of aggregates, in

372 micron-size range, which are capable to deliver the two drugs in combination.
373 LBG was selected because of its potential to enhance macrophage uptake and the
374 amount of polymer was kept purposely high in order to favour internalisation.
375 The morphological observation of LBG-based microparticles, unloaded or drug-
376 loaded, revealed irregular shapes with convoluted surface (Figure 1), without
377 any evident effect resulting from drug association. The latter was actually
378 expected because loadings are relatively low. Similar observations on the
379 morphology and the absence of effect of drug association were reported in a
380 previous work with LBG microparticles associating either INH or RFB
381 separately (Alves et al., 2016).



382

383 **Figure 1.** Microphotographs of LBG-based microparticles viewed by scanning
384 electron microscopy: A) Unloaded LBG microparticles; B) LBG/INH/RFB
385 (10/1/0.5, w/w) microparticles. INH: isoniazid, LBG: locust bean gum, RFB:
386 rifabutin.

387

388 The determined Feret's diameters were rather low, $1.35 \pm 0.7 \mu\text{m}$ for unloaded
389 LBG microparticles and $1.14 \pm 0.51 \mu\text{m}$ for drug-loaded microparticles. Real
390 densities were around 1.4 g/cm^3 and tap densities varied between 0.2 and 0.37
391 g/cm^3 . These values are in the same range of others reported for spray-dried

392 polysaccharide microparticles (Dalpiaz et al., 2015; Pai et al., 2015; Rassu et al.,
393 2015).

394 The encapsulation of both antibiotics was very high, 94% for INH and 102% for
395 RFB, as indicated in Table 1. The resulting loading capacities were, thus, close
396 to theoretical maximum, being of 8.2% and 4.4% for INH and RFB,
397 respectively. Spray-drying is a method usually reported to lead to high efficiency
398 of drug association (Peltonen et al., 2010), as also corroborated in the present
399 work. Moreover, the obtained results are in line with the high association
400 efficiencies reported for each drug when associated individually (Alves et al.,
401 2016).

402 Table 1. Drug association efficiency and loading capacity of
403 LBG/INH/RFB (10/1/0.5, w/w) microparticles (mean \pm SD, n = 3).

Drug	Association efficiency (%)	Loading capacity (%)
INH	94.4 \pm 3.3	8.2 \pm 0.3
RFB	102.1 \pm 1.1	4.4 \pm 0.1

404 INH: isoniazid; RFB: rifabutin

405

406 **3.2. Aerodynamic behaviour of LBG/INH/RFB microparticles**

407 Considering the intended application in lung delivery, the determination of
408 aerosolisation properties stands as the most important aspect in the design of
409 inhalable dry powders. The *in vitro* aerosol performance was determined using a
410 RS01[®] dry powder inhaler and the aerodynamic properties determined upon
411 assessment in the ACI are displayed in Table 2.

412

413

414 Table 2. Aerodynamic characteristics of LBG/INH/RFB (10/1/0.5, w/w)
 415 microparticles (mean \pm SD, n = 3). Loaded powder amount = 22.5 mg,
 416 containing 7.8 mg INH and 3.9 mg RFB, respectively.

Drug	Emitted dose (%)	MMAD (μm)	GSD (μm)	FPD (mg)	FPF (%)
INH	92.6 \pm 0.9	6.2 \pm 0.6	2.4 \pm 0.7	2.7 \pm 0.6	38.0 \pm 1.6
RFB	92.0 \pm 0.5	5.8 \pm 0.3	2.8 \pm 0.2	1.3 \pm 0.1	38.1 \pm 1.8

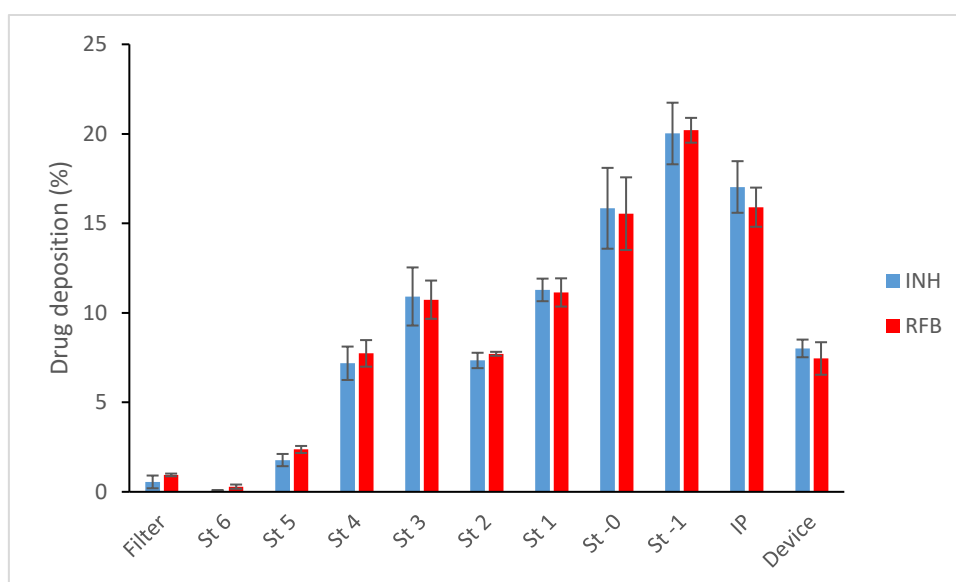
417 FPD: fine particle dose; FPF: fine particle fraction; GSD: geometric standard deviation; INH: isoniazid;
 418 MMAD: mass median aerodynamic diameter; RFB: rifabutin

419

420 The dose emitted from the inhaler was very satisfactory, reaching 92%. This is
 421 indicative of the favourable properties of the material LBG to produce
 422 microparticles by spray-drying with good flowing capacity. However, a
 423 consistent amount of powder impacted on the high stages of the impactor,
 424 leading to MMAD value equal to 5.8 and 6.2 μm for RFB and INH, respectively.
 425 This is due to incomplete deaggregation of microparticle clusters during the
 426 product aerosolisation. It is well known that the aerodynamic performance of a
 427 dry powder inhaler (DPI) is strongly affected by both the device and the
 428 formulation characteristics. However, the spinning movement of the capsule
 429 inside the inhaler used in this study has demonstrated to be the most efficient in
 430 powder deaggregation in comparison with other capsule-based DPI (Martinelli et
 431 al., 2015). Hence, the optimisation of microparticles, with size, shape and
 432 density promoting their aerodynamic behavior will be addressed in the future, in
 433 order to increase the amount of LBG/INH/RFB fine particles capable of reaching
 434 the target site of alveoli. Nevertheless, LBG/INH/RFB microparticles showed a
 435 FPF of 38%, indicating that 38% of the microparticles have aerodynamic
 436 diameter below 5 μm , thus having the necessary conditions to reach the
 437 respiratory zone. This value is in agreement with those usually determined for

438 high doses antibiotic powder formulated without lactose as carrier (Belotti et al.,
439 2015; Maretti et al., 2016).

440 Figure 2 shows the stage-by-stage deposition profiles of both drugs encapsulated
441 in the tested microparticles. The similarity of the profiles indicates that the two
442 drugs were equally co-deposited on the different stages. This supports the
443 decision of developing a carrier with drug combination, as the microparticles
444 demonstrate to have homogeneous composition, leading to a co-deposition of
445 drugs.



446
447 **Figure 2.** Stage-by-stage deposition profiles of isoniazid and rifabutin inside the
448 Andersen cascade impactor after RS01 aerosolisation at 60 L/min, inhalation 4L
449 (values are mean \pm SD, n = 3).

450

451 3.3. *In vitro* drug release from LBG microparticles

452 Release studies were performed in PBS pH 7.4 added of 1% Tween 80[®]. In this
453 way, the local pH of the alveolar zone is resembled, along with the content of
454 surfactant (Kyle et al., 1990), and the dissolution of RFB is ensured (Alves et al.,
455 2016). The release profile determined for each drug is depicted in Figure 3.

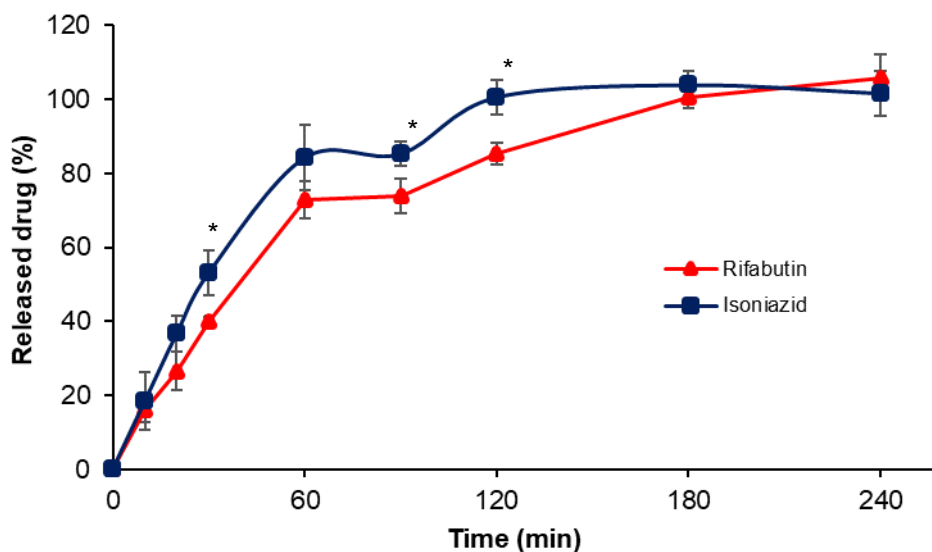


Figure 3. *In vitro* release of isoniazid (INH) and rifabutin (RFB) from LBG/INH/RFB (10/1/0.5, w/w) microparticles, in PBS pH 7.4 - 1% Tween 80® at 37 °C (LBG: locust bean gum; mean ± SD, n = 3). *p < 0.05 comparing release of two drugs.

As can be observed, the release of the drugs is rapid, at 30 min 40% (RFB) – 50% (INH) of the antibiotics being already available. At 60 min, the values reach 73% for RFB and 84% for INH. Although the profile is very similar for both antibiotics, RFB release is somewhat slower than that of INH, with statistically significant differences at some time-points (30, 90 and 120 min, p < 0.05). The higher release of INH is a consequence of its higher solubility in aqueous media (O'Neil, 2006). Considering the conditions of the assay, the rapid release was expected, as LBG is a hydrophilic polymer and rapidly dissolved, releasing the associated drugs. Despite this observation, slower drug release is expected to occur *in vivo*, as has been reported (Bur et al., 2010; Hagi et al., 2014). When reaching the alveoli, microparticles will deposit on an epithelium

481 covered by the lung lining fluid (Fröhlich et al., 2016), which is estimated to
482 have 0.01 – 0.1 μm . In this manner, deposited particles will not be immersed,
483 only a small part being in direct contact with fluid instead and, therefore, erosion
484 and dissolution will initiate from underneath the microparticles (Bur et al., 2010;
485 Haghi et al., 2014). Ultimately, this will result in slower release and is also a
486 relevant observation towards the objective of having particle uptake by
487 macrophages before complete dissolution and drug release.

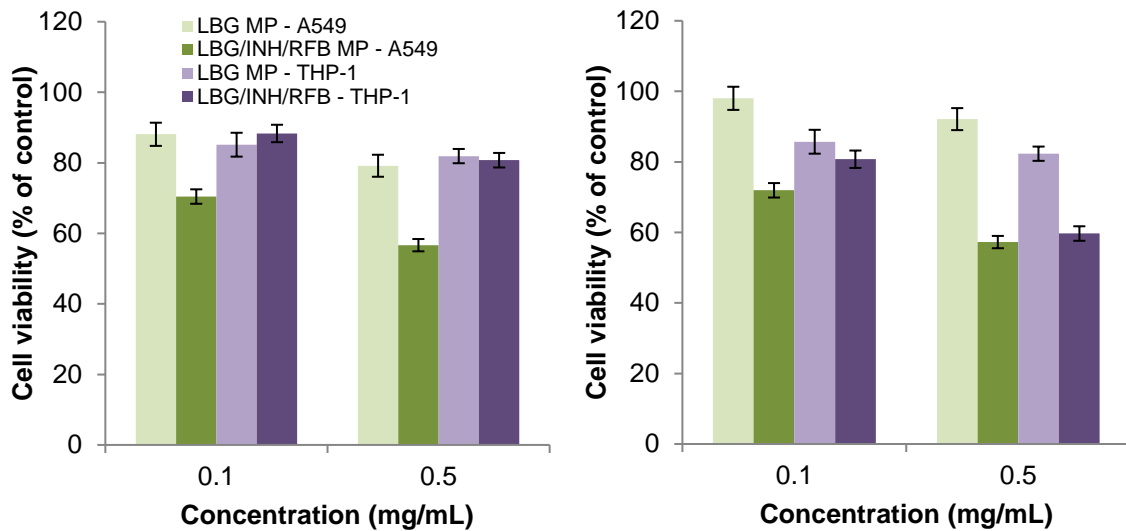
488

489 **3.4. *In vitro* cytotoxicity of LBG microparticles**

490 Two complementary cell viability assays were used to test the effect of
491 LBG/INH/RFB microparticles, the metabolic assay MTT and the LDH release
492 assay, which assesses cell membrane integrity. Considering the environment
493 underlying tuberculosis pathogenesis, alveolar epithelial cells (A549) and
494 macrophage-like cells (macrophage-differentiated THP-1 cells) were used.
495 Microparticle concentrations of 0.1 and 0.5 mg/mL were tested. These are
496 concentrations typically reported in the assessment of lung drug carriers, despite
497 being possibly overestimated if an alveolar area of 100 m^2 is considered
498 (Fröhlich et al., 2016). Unloaded microparticles and free drugs were tested as
499 controls.

500 Regarding the MTT assay, as can be observed in Figure 4A and 4B, the
501 exposure of A549 cells to drug-loaded microparticles induced very similar
502 results after 3 h or 24 h, evidencing an absence of time-dependent effect.
503 However, there is a clear concentration-dependent effect ($p < 0.05$), visible at
504 both time-points, as the resulting cell viability decreases from 72% to 57% (at 24
505 h) as the concentration of microparticles increases from 0.1 to 0.5 mg/mL.

506 Similar observations regarding the effect of time and concentration resulted from
 507 the incubation with unloaded LBG microparticles, although in that case cell
 508 viabilities remained well above the 70% considered the threshold beyond which
 509 a toxic effect is occurring (ISO, 2009).
 510



511
 512 **Figure 4.** A549 and macrophage-like THP-1 cell viability after A) 3 h and B) 24
 513 h exposure to unloaded LBG and LBG/INH/RFB (10/1/0.5, w/w) microparticles
 514 (MP); C) 24 h exposure to INH as free drug and D) 24 h exposure to RFB as free
 515 drug. Data represent mean \pm SEM (n = 3, six replicates per experiment at each
 516 concentration). Dashed line represents 70% cell viability (INH: isoniazid; LBG:
 517 locust bean gum; MP: microparticles; RFB: rifabutin).

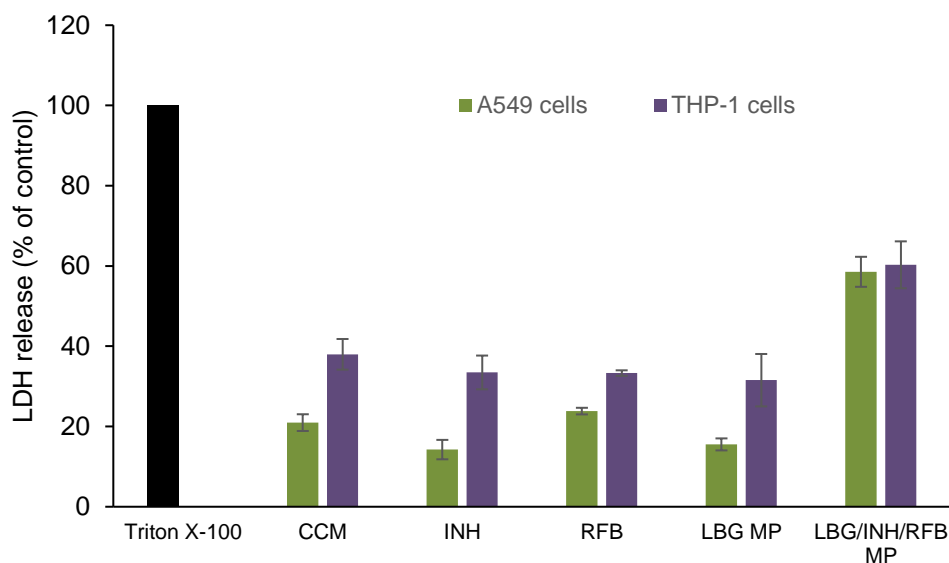
518
 519 Macrophage-differentiated THP-1 cells showed a somewhat different behaviour,
 520 apparently being less sensitive to the contact with drug-loaded microparticles
 521 after short-time exposure (3 h, Figure 4A). Indeed, at that time-point, while
 522 A549 cells registered 57% cell viability for the concentration of 0.5 mg/mL,
 523 macrophage-like THP-1 cells remained at 81%. Nevertheless, the prolongation

524 of the exposure to 24 h (Figure 4B) decreased cell viability to 60%, which is
525 similar to the 57% registered for A549 cells.

526 The results obtained on both cell lines are comparable to those reported for RFB-
527 loaded LBG microparticles in a previous work and the opposite of those
528 obtained for INH-loaded microparticles (Alves et al., 2016). This suggests that
529 the negative effect of drug-loaded microparticles on cell viability is certainly
530 due, at least in part, to the RFB content. The pH of microparticle suspension in
531 cell culture medium that is incubated with cells is around 7.2, so that is not
532 expected to have a negative contribution. As shown in Figure 4C, INH has no
533 effect on cell viability in any of the tested conditions (concentrations, cell lines)
534 at 24 h when exposed as free drug. An exposure of 3 h similarly generated
535 viabilities around 90-100%, not only for INH, but also for RFB (data not
536 shown). In turn, free RFB (Figure 4D) was observed to induce a decrease of
537 A549 cell viability to 65% after 24 h exposure to the higher concentration,
538 which correlates well with the results observed in the same cell line for drug-
539 loaded microparticles, although in that case viability was even lower (57%).
540 However, a different behaviour was observed in THP-1 cells, which viability
541 remained at 85% upon 24 h exposure to the same concentration of free RFB.
542 Several reports on the literature indicate higher susceptibility of A549 cells
543 comparing with THP-1 cells (Lankoff et al., 2012; Singh et al., 2015). This is
544 generally observed in our results, where THP-1 cells frequently show higher cell
545 viability in the same testing conditions. The fact that THP-1 cells have 85% cell
546 viability when exposed to 0.5 mg/mL RFB and then register 60% when exposed
547 to the same amount of antibiotic encapsulated in LBG microparticles, is possibly
548 attributed to the phagocytic capacity of these cells (Lankoff et al., 2012). This

549 characteristic certainly mediates a more intense contact of the cells with RFB,
550 leading to a reduction of cell viability (Lanone et al., 2009). As referred above
551 for A549 cells, unloaded LBG microparticles were also tested as control in
552 macrophage-differentiated THP-1 cells (Figure 4A and B), resulting in cell
553 viabilities above 80% in all cases. Overall, this is a general indication on the
554 absence of any deleterious effect of the polysaccharide on cell viability under the
555 tested conditions.

556 The amount of the cytoplasmic enzyme LDH released after 24 h contact with the
557 higher concentration of microparticles and free drugs was also determined
558 (Figure 5). The results essentially corroborate those of the MTT, with
559 LBG/INH/RFB microparticles having the more intense effect on released LDH,
560 which is similar in both cell lines. The incubation with CCM generated 21%
561 LDH release in A549 cells and 38% in macrophage-differentiated THP-1 cells.
562 The free drugs (INH and RFB) and LBG MP revealed an effect similar to that of
563 the CCM in each cell line, with no significant differences in released LDH. On
564 the contrary, LBG/INH/RFB microparticles induced significantly higher release
565 of LDH in both cell lines, 58% in A549 cells and 60% in THP-1 cells ($p < 0.05$).



566

567 **Figure 5.** LDH released from A549 and macrophage-like THP-1 cells after 24 h
 568 exposure to 0.05 mg/mL isoniazid (INH), 0.025 mg/mL rifabutin (RFB), 0.5
 569 mg/mL of unloaded LBG and LBG/INH/RFB (10/1/0.5, w/w) microparticles
 570 (MP). Cells incubated with cell culture medium (CCM) are the negative control
 571 and Triton-X 100 is the positive control. Data represent mean \pm SEM (n = 3, six
 572 replicates per experiment at each concentration). *p < 0.05 compared to 10%
 573 Triton X-100

574

575 A comparison of results obtained from the MTT and LDH assays shows that the
 576 latter was more sensitive than the former. Drug-loaded LBG microparticles had
 577 stronger impact in released LDH (Figure 5) compared with the effect on
 578 mitochondrial dehydrogenase activity assessed in MTT assay (Figure 4B). Other
 579 studies report similar observations (Braz et al., 2017; Wang et al., 2009) and
 580 several justifications may apply. In fact, the two assays evaluate different aspects
 581 of the interaction between cells and particles. A possible explanation is that
 582 microparticles act as metabolic enhancers (Braz et al., 2017), thus accelerating
 583 MTT conversion into formazan in spite of the lower number of cells (as

584 indicated by the LDH assay), resulting in the overestimation of cell viability. It
585 may also happen that the interaction occurs mostly at the plasma membrane
586 level, causing cell lysis but without reaching intracellular mitochondria (Wang et
587 al., 2009). The latter is however possibly not applicable at least to THP-1 cells,
588 given the phagocytic capacity of these cells.

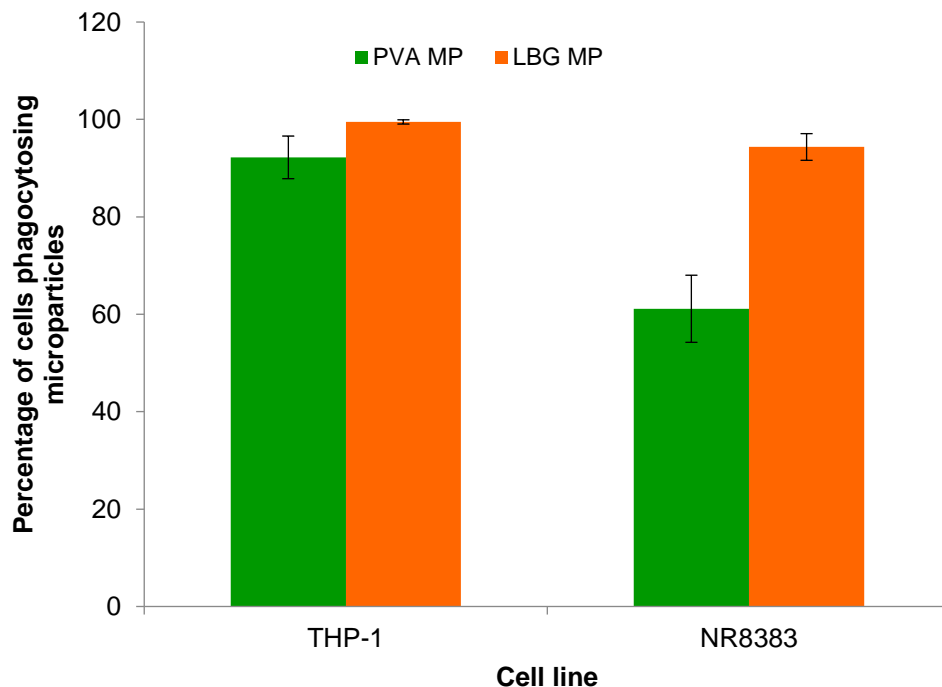
589 The overall observation of cell viability results indicates that the formulation still
590 needs some refinement to improve its toxicological profile. The results are no
591 longer severe as those exhibited with higher amount of rifabutin (Alves et al.,
592 2016), but there is still room for improvement, perhaps by working out a
593 solution that eliminates the use of HCl in the preparation of microparticles.
594 Additionally, the differences observed in the two assays reinforce the need to
595 diversify the range of tests used to obtain a more realistic view of the true impact
596 of the envisioned application.

597

598 **3.5. Uptake of LBG microparticles by macrophage-like cells**

599 Considering the aim of this work, it is very important to evaluate the ability of
600 alveolar macrophages to uptake the produced microparticles. A preliminary
601 study evidenced an uptake around 100% of LBG microparticles independently
602 of the tested dose (50 and 220 $\mu\text{g}/\text{cm}^2$) and used cells (Alves et al., 2016).
603 Considering this high affinity of LBG microparticles for macrophages, the
604 lowest dose (50 $\mu\text{g}/\text{cm}^2$) was selected to provide a comparison of behaviour
605 between LBG and PVA microparticles. The latter were used as control because
606 PVA is not reported to undergo specific recognition by macrophages. Moreover,
607 in order to avoid interference of microparticle size in the uptake, PVA

608 microparticles were tailored to have size similar to LBG microparticles (Ferret's
609 diameter was calculated as $1.5 \pm 1.0 \mu\text{m}$).
610 As depicted in Figure 6, very high macrophage uptake (95-100%) was observed
611 for LBG microparticles in both cell lines. In turn, PVA microparticles induced
612 high uptake (92%) in macrophage differentiated THP-1 cells, but this value
613 decreased significantly to 60% ($p < 0.05$) in rat alveolar macrophages (NR 8383
614 cells). In that case, the uptake was significantly lower than that induced by LBG
615 microparticles ($p < 0.05$), showing a higher affinity of the cells for LBG.



616
617 **Figure 6.** Uptake of fluorescently-labelled locust bean gum (LBG) and
618 polyvinyl alcohol (PVA) microparticles by macrophage-differentiated THP-1
619 cells and NR8383 cells upon 2 h exposure to $50 \mu\text{g}$ microparticles/ cm^2 , at 37°C .
620 Results are expressed as mean \pm SEM ($n \geq 3$).
621
622 Macrophages have a natural ability to uptake particulate matter (Pacheco et al.,
623 2013; Patel et al., 2015) and, thus, the uptake of a certain amount of particles

624 was expected in any case, independently of the particle composition. LBG is,
625 however, a galactomannan, being composed of mannose and galactose units.
626 These are reported to mediate favourable recognition by macrophage surface C-
627 type lectin receptors (Chavez-Santoscoy et al., 2012; Coombs et al., 2006; East
628 and Isacke, 2002).

629 NR8383 cells are reported to naturally express a functional mannose receptor in
630 culture (Vigerust et al., 2012). Therefore, the different response of these cells to
631 the two formulations of microparticles is possibly due to a higher affinity for
632 LBG, mediated by the specific receptor recognition of LBG residues. On the
633 contrary, THP-1 cells differentiated by PMA adopt an activation state of M0
634 which has been reported to not express the mannose receptor (Daigneault et al.,
635 2010). The inability to differentiate between both polymers is, therefore, the
636 possible reason for the similar capture of the two microparticle types.

637

638 **4. Conclusions**

639 In this work, LBG microparticles loaded with a combination of the first-line
640 antitubercular drugs isoniazid and rifabutin were proposed as inhalable carriers
641 for tuberculosis therapy. The co-encapsulation of the drugs in a single carrier
642 meets WHO requirements regarding combined tuberculosis therapy. Drug
643 release from microparticles was fast, but this is expected to be counterbalanced
644 by the reduced amount of fluid in the alveolar zone in *in vivo* conditions. The
645 experimental assessment of aerosolisation properties of LBG microparticles
646 demonstrated a favorable respirable dose lower than 5 μm , albeit the extrafine
647 dose potentially capable of reaching the target alveolar zone should be enhanced
648 in order to maximise macrophage uptake. A preferential ability of rat

649 macrophages to uptake LBG microparticles in comparison with a control was
650 observed *in vitro*, an effect attributed to the presence of mannose and galactose
651 units in LBG. The cytotoxic evaluation of these microparticles demonstrated
652 moderate decrease of cell viability to around 60%, indicating the need to
653 improve this aspect. Overall, the proposed strategy of dual antibiotherapy of
654 tuberculosis mediated by inhalable LBG microparticles is believed to be a
655 promising approach in the treatment of the disease.

656

657 **Acknowledgements**

658 This work was supported by National Portuguese funding through FCT -
659 Fundação para a Ciência e a Tecnologia, through projects PTDC/DTP-
660 FTO/0094/2012, UID/BIM/04773/2013, UID/Multi/04326/2013,
661 UID/QUI/00100/2013, and PEst-OE/QUI/UI4023/2011. The studentship of
662 Susana Rodrigues is also acknowledged (SFRH/BD/52426/2013).

663 The authors also would like to thank Plastiapae Spa (Lecco, Italy) and Qualicaps
664 (Madrid, Spain) for kindly donating the RS01 dry powder inhaler and HPMC
665 capsules, respectively.

666

667 **References**

668 Ahsan, F., Rivas, I.P., Khan, M.A., Torres Suárez, A.I., 2002. Targeting to
669 macrophages: role of physicochemical properties of particulate carriers—
670 liposomes and microspheres—on the phagocytosis by macrophages. *Journal of*
671 *Controlled Release* 79, 29-40.

672 Alkhayat, A.H., Kraemer, S.A., Leipprandt, J.R., Macek, M., Kleijer, W.J.,
673 Friderici, K.H., 1998. Human β -mannosidase cDNA characterization and first

674 identification of a mutation associated with human β -mannosidosis. *Human*
675 *Molecular Genetics* 7, 75-83.

676 Alves, A., Cavaco, J., Guerreiro, F., JLourenço, J., Rosa da Costa, A., Grenha,
677 A., 2016. Inhalable antitubercular therapy mediated by locust bean gum
678 microparticles *Molecules* 21, 1-22.

679 Belotti, S., Rossi, A., Colombo, P., Bettini, R., Rekkas, D., Politis, S., Colombo,
680 G., Balducci, A.G., Buttini, F., 2015. Spray-dried amikacin sulphate powder for
681 inhalation in cystic fibrosis patients: The role of ethanol in particle formation.
682 *European Journal of Pharmaceutics and Biopharmaceutics* 93, 165-172.

683 Braz, L., Grenha, A., Ferreira, D., Rosa da Costa, A.M., Gamazo, C., Sarmiento,
684 B., 2017. Chitosan/sulfated locust bean gum nanoparticles: In vitro and in vivo
685 evaluation towards an application in oral immunization. *Int J Biol Macromol* 96,
686 786-797.

687 Bur, M., Huwer, H., Muys, L., Lehr, C.-M., 2010. Drug transport across
688 pulmonary epithelial cell monolayers: Effects of particle size, apical liquid
689 volume, and Deposition technique. *Journal of Aerosol Medicine and Pulmonary*
690 *Drug Delivery* 23, 119-127.

691 Buttini, F., Colombo, G., Kwok, P.C.L., Wui, W.T., 2013. *Aerodynamic*
692 *Assessment for Inhalation Products: Fundamentals and Current Pharmacopoeial*
693 *Methods, Inhalation Drug Delivery*. John Wiley & Sons, Ltd, pp. 91-119.

694 Chavez-Santoscoy, A.V., Roychoudhury, R., Pohl, N.L.B., Wannemuehler, M.J.,
695 Narasimhan, B., Ramer-Tait, A.E., 2012. Tailoring the immune response by
696 targeting C-type lectin receptors on alveolar macrophages using “pathogen-like”
697 amphiphilic polyanhydride nanoparticles. *Biomaterials* 33, 4762-4772.

698 Coombs, P., Taylor, M., Drickamer, K., 2006. Two categories of mammalian
699 galactose-binding receptors distinguished by glycan array profiling.
700 *Glycobiology* 16, 1C-7C.

701 Daigneault, M., Preston, J., Marriott, H., Whyte, M., Dockrell, D., 2010. The
702 identification of markers of macrophage differentiation in PMA-stimulated
703 THP-1 cells and monocyte-derived macrophages. *PLoS ONE* 5, e8668.

704 Dalpiaz, A., Fogagnolo, M., Ferraro, L., Capuzzo, A., Pavan, B., Rassa, G.,
705 Salis, A., Giunchedi, P., Gavini, E., 2015. Nasal chitosan microparticles target a
706 zidovudine prodrug to brain HIV sanctuaries. *Antiviral Research* 123, 146-157.

707 East, L., Isacke, C.M., 2002. The mannose receptor family. *Biochimica et*
708 *Biophysica Acta (BBA) - General Subjects* 1572, 364-386.

709 EMA, 2014. Guideline on quality of oral modified release products. European
710 Medicines Agency, pp. 1-16.

711 Fröhlich, E., Mercuri, A., Wu, S., Salar-Behzadi, S., 2016. Measurements of
712 deposition, lung surface area and lung fluid for simulation of inhaled
713 compounds. *Frontiers in Pharmacology* 7, 181.

714 Grenha, A., Seijo, B., Remuñán-López, C., 2005. Microencapsulated chitosan
715 nanoparticles for lung protein delivery. *European Journal of Pharmaceutical*
716 *Sciences* 25, 427-437.

717 Gupta, A., Meena, J., Sharma, D., Gupta, P., Gupta, U.D., Kumar, S., Sharma,
718 S., Panda, A.K., Misra, A., 2016. Inhalable particles for “Pincer Therapeutics”
719 targeting nitazoxanide as bactericidal and host-directed agent to macrophages in
720 a mouse model of tuberculosis. *Molecular Pharmaceutics* 13, 3247-3255.

721 Haghi, M., Ong, H.X., Traini, D., Young, P., 2014. Across the pulmonary
722 epithelial barrier: Integration of physicochemical properties and human cell

723 models to study pulmonary drug formulations. *Pharmacology & Therapeutics*
724 144, 235-252.

725 Hiremath, P.S., Saha, R.N., 2008. Controlled release hydrophilic matrix tablet
726 formulations of isoniazid: design and in vitro studies. *AAPS PharmSciTech* 9,
727 1171-1178.

728 ISO, 2009. Biological evaluation of medical devices Part 5: Tests for in vitro
729 cytotoxicity, in: Standardization, I.O.f. (Ed.), 10993-5.

730 Kaur, M., Garg, T., Narang, R.K., 2016. A review of emerging trends in the
731 treatment of tuberculosis. *Artificial Cells, Nanomedicine, and Biotechnology* 44,
732 478-484.

733 Kyle, H., Ward, J., Widdicombe, J., 1990. Control of pH of airway surface liquid
734 of the ferret trachea in vitro. *Journal of Applied Physiology* 68, 135-140.

735 Lankoff, A., Sandberg, W.J., Wegierek-Ciuk, A., Lisowska, H., Refsnes, M.,
736 Sartowska, B., Schwarze, P.E., Meczynska-Wielgosz, S., Wojewodzka, M.,
737 Kruszewski, M., 2012. The effect of agglomeration state of silver and titanium
738 dioxide nanoparticles on cellular response of HepG2, A549 and THP-1 cells.
739 *Toxicology Letters* 208, 197-213.

740 Lanone, S., Rogerieux, F., Geys, J., Dupont, A., Maillot-Marechal, E.,
741 Boczowski, J., Lacroix, G., Hoet, P., 2009. Comparative toxicity of 24
742 manufactured nanoparticles in human alveolar epithelial and macrophage cell
743 lines. *Particle and Fibre Toxicology* 6, 1-12.

744 Lee, W.-H., Loo, C.-Y., Traini, D., Young, P.M., 2015. Nano- and micro-based
745 inhaled drug delivery systems for targeting alveolar macrophages. *Expert*
746 *Opinion on Drug Delivery* 12, 1009-1026.

747 Maretti, E., Rustichelli, C., Romagnoli, M., Balducci, A.G., Buttini, F.,
748 Sacchetti, F., Leo, E., Iannuccelli, V., 2016. Solid lipid nanoparticle assemblies
749 (SLNas) for an anti-TB inhalation treatment: A Design of Experiments approach
750 to investigate the influence of pre-freezing conditions on the powder
751 respirability. *International Journal of Pharmaceutics* 511, 669-679.

752 Martinelli, F., Balducci, A.G., Rossi, A., Sonvico, F., Colombo, P., Buttini, F.,
753 2015. "Pierce and inhale" design in capsule based dry powder inhalers: Effect of
754 capsule piercing and motion on aerodynamic performance of drugs. *International*
755 *Journal of Pharmaceutics* 487, 197-204.

756 McBryde, E.S., Meehan, M.T., Doan, T.N., Ragonnet, R., Marais, B.J.,
757 Guernier, V., Trauer, J.M., 2017. The risk of global epidemic replacement with
758 drug resistant M. tuberculosis strains. *International Journal of Infectious*
759 *Diseases* 56, 14-20.

760 NICE, 2016. NICE guideline for tuberculosis, in: Excellence, N.I.f.H.a.C. (Ed.),
761 London.

762 O'Neil, M., 2006. *The Merck Index: An encyclopedia of chemicals, drugs, and*
763 *biologicals*, 14 ed, New Jersey.

764 Pacheco, P., White, D., Sulchek, T., 2013. Effects of microparticle size and Fc
765 density on macrophage phagocytosis. *PLoS ONE* 8, e60989.

766 Pai, R.V., Jain, R.R., Bannalikal, A.S., Menon, M.D., 2015. Development and
767 evaluation of chitosan microparticles based dry powder inhalation formulations
768 of rifampicin and rifabutin. *Journal of Aerosol Medicine and Pulmonary Drug*
769 *Delivery* 29, 179-195.

770 Parumasivam, T., Chang, R.Y.K., Abdelghany, S., Ye, T.T., Britton, W.J., Chan,
771 H.-K., 2016. Dry powder inhalable formulations for anti-tubercular therapy.
772 *Advanced Drug Delivery Reviews* 102, 83-101.

773 Patel, B., Gupta, N., Ahsan, F., 2015. Particle engineering to enhance or lessen
774 particle uptake by alveolar macrophages and to influence the therapeutic
775 outcome. *European Journal of Pharmaceutics and Biopharmaceutics* 89, 163-
776 174.

777 Peltonen, L., Valo, H., Kolakovic, R., Laaksonen, T., Hirvonen, J., 2010.
778 Electro spraying, spray drying and related techniques for production and
779 formulation of drug nanoparticles. *Expert Opinion on Drug Delivery* 7, 705-719.
780 Ph.Eur., 2014. *European Pharmacopoeia*, in: Medicines, E.D.f.t.Q.o. (Ed.).

781 Pollard, M., Kelly, R., Fischer, P., Windhab, E., Eder, B., Amadò, R., 2008.
782 Investigation of molecular weight distribution of LBG galactomannan for flours
783 prepared from individual seeds, mixtures, and commercial samples. *Food Hyd.*
784 22, 1596–1606.

785 Rassa, G., Soddu, E., Cossu, M., Brundu, A., Cerri, G., Marchetti, N., Ferraro,
786 L., Regan, R.F., Giunchedi, P., Gavini, E., Dalpiaz, A., 2015. Solid
787 microparticles based on chitosan or methyl- β -cyclodextrin: A first formulative
788 approach to increase the nose-to-brain transport of deferoxamine mesylate.
789 *Journal of Controlled Release* 201, 68-77.

790 Singh, M., Bhatnagar, P., Mishra, S., Kumar, P., Shukla, Y., Gupta, K.C., 2015.
791 PLGA-encapsulated tea polyphenols enhance the chemotherapeutic efficacy of
792 cisplatin against human cancer cells and mice bearing Ehrlich ascites carcinoma.
793 *International Journal of Nanomedicine* 10, 6789-6809.

794 USP, 2015. United States Pharmacopeia USP-38, in: Convention, U.S.P. (Ed.),
795 Rockville.

796 Vigerust, D., Vick, S., Shepherd, V., 2012. Characterization of functional
797 mannose receptor in a continuous hybridoma cell line. BMC Immunology 13, 1-
798 13.

799 Wang, C., Muttill, P., Lu, D., Beltran-Torres, A., Garcia-Contreras, L., Hickey,
800 A., 2009. Screening for potential adjuvants administered by the pulmonary route
801 for tuberculosis vaccines. The AAPS Journal 11, 139-147.

802 Wells, B., Dipiro, J., Schwinghammer, T., Dipiro, C., 2009. Tuberculosis,
803 Pharmacotherapy Handbook, 9 ed. McGraw-Hill, p. 1066.

804 WHO, 2014. The End TB Strategy. World Health Organization, Geneva.

805 WHO, 2016 Global Tuberculosis Report 2016. World Health Organization,
806 Geneva.

807

808